Revisited Yule–Nielsen model without fitting of the n parameter

Serge Mazauric, Mathieu Hébert, Thierry Fournel

▶ **To cite this version:**

Serge Mazauric, Mathieu Hébert, Thierry Fournel. Revisited Yule–Nielsen model without fitting of the n parameter. Journal of the Optical Society of America. A Optics, Image Science, and Vision, 2018, 35 (2), 10.1364/JOSAA.35.000244 . hal-01691409

HAL Id: hal-01691409
https://hal.science/hal-01691409

Submitted on 26 Jan 2018

HAL is a multi-disciplinary open access archive for the deposit and dissemination of scientific research documents, whether they are published or not. The documents may come from teaching and research institutions in France or abroad, or from public or private research centers.

L'archive ouverte pluridisciplinaire **HAL**, est destinée au dépôt et à la diffusion de documents scientifiques de niveau recherche, publiés ou non, émanant des établissements d'enseignement et de recherche français ou étrangers, des laboratoires publics ou privés.

Revisited Yule-Nielsen model without fitting of the n parameter

SERGE MAZAURIC[1,2,*], MATHIEU HÉBERT[1], AND THIERRY FOURNEL[1]

[1] Université de Lyon, Université Jean Monnet de Saint-Etienne, CNRS UMR 5516 Laboratoire Hubert Curien, F-42000 Saint-Etienne, France
[2] CPE Lyon, Domaine Scientifique de la Doua, 43 boulevard du 11 Novembre 1918 BP 82077 - 69616 Villeurbanne Cedex
[*] Corresponding author: serge.mazauric@univ-st-etienne.fr

Compiled January 26, 2018

We introduce a so-called "Mean-Path-Defined Yule-Nielsen" (MPD-YN) model for predicting the color of halftone prints in reflectance or transmittance modes, inspired of the Yule-Nielsen modified Spectral Neugebauer model, where the empirical n value is replaced with a spectral parameter different for each halftone, directly calculated thanks to a closed-form formula, function of the measured spectral reflectances (or accordingly transmittances) of fulltone calibration patches and the surface coverages of the Neugebauer primaries in the halftone. This parameter is based on the average number of internal reflections undergone by light between two half-layers of the print, whose expression derives from a flux transfer model between the two half-layers. According to the tests carried out in this study with paper printed in inkjet, the predictive performances of the MPD-YN model are rather good and very close to those obtained with the Yule-Nielsen model. © 2018 Optical Society of America

OCIS codes: (000.3860) Mathematical methods in physics, (120.5700) Reflection, (120.7000) Transmission, (230.4170) Multilayers, (100.2810) Halftone image reproduction

http://dx.doi.org/10.1364/ao.XX.XXXXXX

1. INTRODUCTION

Spectral prediction models are key tools for fast and accurate color management in printing. They are also indispensable for designing advanced printing features such as those where the print displays different images according to the viewing conditions. Such multi-view effects can be obtained by using metallic inks [1] or a specular support [2] and observing the print in or out of the specular reflection direction. They can also be obtained by double-side printing with classical inks and supports, by observing one face in reflection mode or both faces simultaneously in transmission mode [3–5]. For these printing configurations, color management based on digital methods like ICC profile is almost impossible because the number of needed sample measurements, often beyond one thousand for single-mode observation, exponentially increases with the number of observation modes. The calibration time of the printing system thus becomes inacceptable, whereas a few tens of measurements often suffice to calibrate a prediction model, thus allowing the prediction of all reproducible colors in the different modes.

Inside a diffusing medium printed in halftone, the light propagates laterally from one ink dot to other ones by multiple internal reflections before exiting the print, which makes the reflectance of the halftone darker than it would be in absence of these internal reflections. This phenomenon is often called Yule-Nielsen effect, or "optical dot gain". Even though it has been established that this phenomenon is more or less pronounced according to the point spread function of the support and the halftone screen frequency [6], no simple model has been able yet to provide precise relationship between the phenomenon and these parameters. However, despite its simplicity, the Yule-Nielsen modified Neugebauer equation (or simply Yule-Nielsen equation) [7, 8] allows accurate predictions of the spectral reflectance of halftone prints on various diffusing or transparent supports. The optical dot gain is modeled by an empirical n parameter fitted from a few tens of halftones used for the calibration of the model. This model belongs, together with the spectral Neugebauer model, to the category of "surface models" as defined in Ref. [9]. They do not offer the possibility of varying the measurement geometry, or the ink layer thickness, which must be identical for the calibration and the prediction.

Another category of spectral reflectance prediction models for prints is the "phenomenological models". They are more complex since they intend to describe explicitly the optical dot gain thanks to flux transfers between the layers of the print, taking into account physical considerations such as the change of refractive index between air and the diffusing medium, or the lighting and observation geometries: this is the case of the Clapper-Yule model [10] or the Duplex Primary Reflectance-Transmittance model [11], which take into account the multiple

reflections of light when it propagates between the interface and the support through the ink layers.

The present study merges the two approaches since we propose a surface model similar to the Yule-Nielsen model, but without fitted n parameter. This latter is replaced with a spectral parameter different for each halftone, corresponding to the average number of internal reflections between two sublayers of the print (the upper and the lower half layers), which depends on the spectral reflectances and transmittances of the primaries, thereby on their absorbance, and their respective surface coverages. Our model, called "Mean-Path-Defined Yule-Nielsen" (MPD-YN), maintains the famous Yule-Nielsen equation, appreciable for its simplicity, while removing the determination step for the n value. In contrast with the Yule-Nielsen model, however, the spectral transmittance of the unprinted support needs to be measured.

This model is part of a series of studies whose objective is to predict both reflectance and transmittance of single-side and duplex prints, by targeting as good accuracy as the numerous reflectance prediction models for single-side prints, and by trying to increase as little as possible the number of color patches to be printed for calibration of the reflectance and transmittance model in comparison to those needed by reflectance only-models (e.g., 44 patches in Ref. [13]). In the case of duplex prints, the process of minimizing the number of calibration patches is crucial because the number of duplex color pairs to predict is the square of the number of single-side colors that the reflectance models usually have to predict.

Before presenting the MPD-YN model, we first recall in Section 2 the Yule-Nielsen model and we discuss its advantages and limitations. The MPD-YN model relies on a flux transfer approach and the subdivision of the print into two half-layers. The matrix formalism associated with the flux transfer model, introduced in Refs. [11] and [12], is recalled in Section 3 and used to calculate the average number of internal reflections between two layers. The MPD-YN model is presented in detail in Section 4 for reflectance predictions and in Section 5 for transmittance predictions. Its extension to duplex halftone prints is presented in Section 6. The method for assessing the mechanical dot gain in halftone print is described in Section 7: this method, proposed by Hersch and Crété [13], relies on ink spreading functions giving the correspondence between nominal and effective surface coverages and taking into account the fact that an ink may spread differently on the paper or on top of another ink. An experimental verification of the model is presented in Section 8 and our conclusions are finally drawn in Section 9.

2. YULE-NIELSEN MODEL

Let us consider a CMY halftone color printed on a diffusing medium. It can be seen as a mosaic of the height Neugebauer primaries, obtained when superposing cyan, magenta and yellow halftone screens: white (surface with no ink, labelled $i = 1$), cyan, magenta, yellow, red (magenta + yellow), green (cyan + yellow), blue (cyan + magenta) and black (cyan + magenta + yellow). We denote as a_i $(i = 1, ..., 8)$ the surface coverages of the Neugebauer primaries. They are obtained from the surface coverages of the cyan, magenta and yellow inks using Demichel's equations [14] valid for most types of typical stochastic halftoning techniques or cluster dot halftoning when the halftone screens of the different channels have appropriate orientations [9]:

$$\begin{aligned} a_1 &= (1-c)(1-m)(1-y) \\ a_2 &= c(1-m)(1-y) \\ a_3 &= (1-c)m(1-y) \\ a_4 &= (1-c)(1-m)y \\ a_5 &= (1-c)my \\ a_6 &= c(1-m)y \\ a_7 &= cm(1-y) \\ a_8 &= cmy \end{aligned} \tag{1}$$

Within a halftone print, light propagates laterally from one area to another one before exiting the medium, thus meeting various primaries, a phenomenon called "optical dot gain" or Yule-Nielsen effect [7, 8]. This phenomenon is modeled empirically by the introduction in the Neugebauer formula of a free parameter n, yielding the Yule-Nielsen modified Neugebauer reflectance formula:

$$R(\lambda) = \left[\sum_{i=1}^{8} a_i R_i(\lambda)^{1/n} \right]^n \tag{2}$$

where R_i are the reflectance factors of the solid Neugebauer primaries. The parameter n is fitted in order to minimize the mean square deviation between measured and predicted spectra of calibration samples. A version of the Yule-Nielsen model transposed to the transmission factor has been proposed in Ref. [15] with similar performence as for reflectance predictions, for both single-sided prints and duplex prints.

In absence of scattering within the printing support (very specular substrates), the n value is theoretically equal to (or very close to) 1. However, we experimentally observe that its optimal value, fitted in order to obtain the best agreement between measured and predicted spectral reflectances for a set of patches, is rather close to 2 for transparent films because of the slight light scattering by the inks [16]. When the scattering in the support increases, the n value generally increases too (the Yule-Nielsen effect is stronger): it can reach 10 for certain paper prints [9], and can even tend asymptotically to infinity [3]. It can also take negative values, especially when the ink penetrates deeply into the paper [17–19]. When the halftone screen frequency increases, an increase of the n value is often observed [20], which can be explained by the fact that the ink dots are smaller and closer to each other, or equivalently by the fact that the halftone screen period decreases in respect to the average distance of lateral propagation of light within the support, which can be deduced from the point spread function of the support itself [9].

The Yule-Nielsen model is simple and efficient, but the introduction of the fitted n parameter to empirically model the optical dot gain does not really find simple interpretation. Various attempts to find a physical justification have been proposed. Some authors have modeled the transition probabilities between primaries [21–23], other ones have modeled the light reflection by the print using the convolution of a spectral transmission surface function associated with the ink layer and the point spread function describing the scattering of light in paper substrates [24]. In Refs. [6, 25, 26] Rogers used this convolution approach to derive, from the radiative transfer theory, the Yule-Nielsen equation with a value of n approaching 2 as the substrate becomes a perfect diffuser, which is in contradiction with the experimentally observed values. This theoretical model, which is also very

elegant, is rather difficult to implement because it needs high computation times and also requires to take into account the actual shape of the ink dots.

Finally, the Yule-Nielsen model assumes that the fitted n parameter is independent of the wavelength and the Neugebauer primaries, whatever their absorbance are. However, when light encounters a very absorbing primary, it is strongly attenuated and its average path is consequently shortened; average light paths therefore depends on the spectral absorbance of the primaries. We propose in this work to review the Yule-Nielsen model in which the n parameter is a spectral quantity calculated from the measured spectra for a selection of calibration samples and no longer a fitted parameter minimizing the distance between predicted and measured spectra.

3. FLUX TRANSFERS AND AVERAGE NUMBER OF INTERNAL REFLECTIONS

The purpose of this section is to recall the bases of the discrete two-flux model and its matrix formalism, applied to a stack of two layers, from which we can then calculate the mean free path of light, in the form of an average number of internal reflections between the two layers.

A flux transfer model is particularly adapted to the layered structure of printed supports. When the printing support is strongly scattering, like paper or white polymer, we can use a two-flux model. The model presented in Ref. [11] applies with a stack of layers of strongly diffusing materials and the interfaces between them. Each component, layer or interface, is characterized by four transfer factors: the front-side reflectance r, the back-side reflectance r', the forward transmittance t and the backward transmittance t'. The component is said to be symmetrical when $r = r'$, and $t = t'$. All fluxes and transfer factors may also depend upon wavelength. When two components are on top of each other, inter-reflections of light occur between them, thus producing mutual exchanges between the fluxes propagating forwards (denoted as i_k in Fig. 1) and backwards (denoted as j_k). These exchanges can be easily described by using flux transfer matrices. For each component $k = 1$ or 2, assuming $t_k \neq 0$, the relations between forward and backward fluxes is described by the following matrix equation:

$$\begin{pmatrix} i_{k-1} \\ j_{k-1} \end{pmatrix} = \frac{1}{t_k} \begin{pmatrix} 1 & -r'_k \\ r_k & t_k t'_k - r_k r'_k \end{pmatrix} \begin{pmatrix} i_k \\ j_k \end{pmatrix} \quad (3)$$

where the matrix is the transfer matrix attached to the component k, denoted as $\mathbf{M}_k$:

$$\mathbf{M}_k = \frac{1}{t_k} \begin{pmatrix} 1 & -r'_k \\ r_k & t_k t'_k - r_k r'_k \end{pmatrix} \quad (4)$$

Grouping components 1 and 2 together, Eq. (3) can be repeated twice. One obtains:

$$\begin{pmatrix} i_0 \\ j_0 \end{pmatrix} = \mathbf{M_1} \begin{pmatrix} i_1 \\ j_1 \end{pmatrix} = \mathbf{M_1 M_2} \begin{pmatrix} i_2 \\ j_2 \end{pmatrix} = \mathbf{M} \begin{pmatrix} i_2 \\ j_2 \end{pmatrix} \quad (5)$$

where $\mathbf{M}$, product of the transfer matrices of the individual components, is the transfer matrix representing the two layers together, similarly defined as Eq. (4) in terms of its transfer factors R, T, R' and T'. The multiplicative property of transfer matrices is true for any number of components, and the left-to-right position of the matrices in the product reproduces the front-to-back position of the corresponding components. Every transfer matrix has the structure displayed in Eq. (4) and from a given transfer matrix $\mathbf{M} = (m_{ij})$, provided $m_{11} \neq 0$, one retrieves the transfer factors in the following way:

$$R = m_{21}/m_{11} \quad (6)$$

$$T = 1/m_{11} \quad (7)$$

$$R' = -m_{12}/m_{11} \quad (8)$$

$$T' = \det \mathbf{M}/m_{11} = m_{22} - m_{21}m_{12}/m_{11} \quad (9)$$

Applying formulas (6) to (9) to the matrix $\mathbf{M_1 M_2}$ [see Eq. (5)] representing the stack of layers displayed in Fig. 1 yields:

$$R = r_1 + \frac{t_1 t'_1 r_2}{1 - r'_1 r_2} \quad (10)$$

$$T = \frac{t_1 t_2}{1 - r'_1 r_2} \quad (11)$$

$$R' = r'_2 + \frac{t_2 t'_2 r'_1}{1 - r'_1 r_2} \quad (12)$$

$$T' = \frac{t'_1 t'_2}{1 - r'_1 r_2} \quad (13)$$

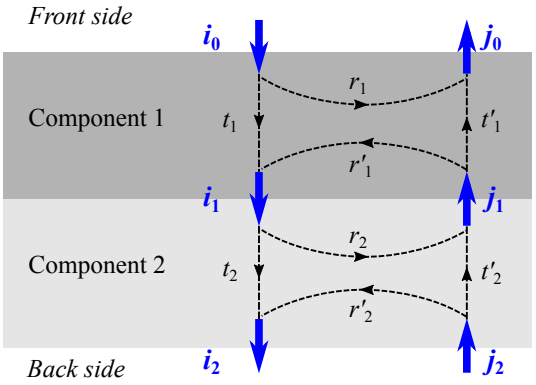

Fig. 1. Flux transfers between two planar components (arrows do not render orientation of light).

Another way of obtaining formulas (10) to (13) is the method used by Kubelka, who, in his study of non-symmetric diffusing media [27], considered all possible paths of light following multiple reflections between the two layers (see Fig. 2). Let us detail the calculations allowing to obtain the equation of the front-side reflectance given by Eq. (10). We consider light that is internally reflected a number of times before leaving the interface between the two layers. Light can be internally reflected one time and exit, three times and exit, ... $2k+1$-times and exit. At the first internal reflection, light is attenuated by r_2. At the thirth internal reflections, light is further attenuated by $r'_1 r_2$, and finally, at the $2k+1$ *th* internal reflection, light is attenuated by $r_2 (r'_1 r_2)^k$. The sum of all the possible paths for light leads to convergent geometric series:

$$R = r_1 + t_1 t'_1 \sum_{k=0}^{\infty} r_2 \left(r'_1 r_2\right)^k = r_1 + \frac{t_1 t'_1 r_2}{1 - r'_1 r_2} \quad (14)$$

We observe that before being reflected, a light ray undergoes an odd number of internal reflections between the two layers: k reflections on the inner face of layer 1 and $k+1$ reflections on

the upper face of layer 2, which therefore makes $2k+1$ internal reflections and a global factor $r_1'^k r_2^{k+1}$. It is thus possible to deduce the average number of internal reflections undergone by light component before exiting the medium at the upper side. This number, denoted n_R, is the average of the odd numbers $2k+1$, with $k \in \mathbb{N}$, weighted by $r_1'^k r_2^{k+1}$, which is the probability for light to undergo an odd number of internal reflections. Thus one can write:

$$n_R = \frac{1 \times r_2 + 3 \times r_1' r_2^2 + 5 \times r_1'^2 r_2^3 + ... + (2k+1) \times r_1'^k r_2^{k+1} + ...}{r_2 + r_1' r_2^2 + r_1'^2 r_2^3 + ... + r_1'^k r_2^{k+1} + ...} \tag{15}$$

Then, by denoting $q = r_1' r_2$, Eq. (15) can be written:

$$n_R = \frac{r_2 \sum_{k=0}^{\infty} (2k+1)\, q^k}{r_2 \sum_{k=0}^{\infty} q^k} \tag{16}$$

which yields

$$n_R = 1 + 2q \frac{\sum_{k=1}^{\infty} k q^{k-1}}{\sum_{k=0}^{\infty} q^k} \tag{17}$$

The lower term of the fraction of Eq. (17) is the geometric serie with the common ratio q; its limit is $1/(1-q)$. The upper term is the first derivative of the geometric serie with the common ratio q, it converges to the derivative of the geometric serie, i.e. $1/(1-q)^2$. Finally, one obtains:

$$n_R = 1 + \frac{2q}{1-q} = \frac{1+q}{1-q} = \frac{1 + r_1' r_2}{1 - r_1' r_2} \tag{18}$$

The average number of reflections n_R is the number of reflections that would yield the same attenuation of light as in the present case, if at each reflection cycle, the attenuation of light would be only $r_1' r_2$. This means that we transform the "multiple internal reflections" into a series of serial attenuation filters having each an attenuation of $r_1' r_2$ and ask how many of these filters we need to obtain the same attenuation of light as with two layer having an infinite number of internal reflections.

Likewise, the average number of internal reflections undergone by light before exiting the medium on the back side is:

$$n_T = n_R - 1 = \frac{2 r_1' r_2}{1 - r_1' r_2} \tag{19}$$

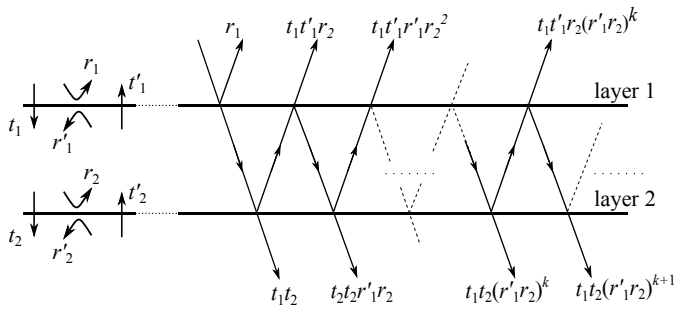

Fig. 2. Reflections and transmissions between two diffusing layers.

4. MEAN-PATH-DEFINED YULE-NIELSEN (MPD-YN) MODEL IN REFLECTANCE MODE

Let us come back to the Yule-Nielsen model, by starting with the physical interpretation of this model that we introduced in Ref. [3]. We noticed that the Yule-Nielsen equation can be formally derived by modelling the reflectance of the halftone print as the result of the reflection by the support and n events of spectral filtering due to the Neugebauer primaries in respect to their respective surface coverage, these filtering events being separated by n scattering events that make light moving from one primary to any other primary. This interpretation implicitly assumes that this number of scattering events, the same for all primaries and all wavelengths of light, correlates with the lateral propagation of light into the print, which is admitted to be at the origin of the Yule-Nielsen effect. We now refine this interpretation by considering that the number of scattering events, thereby the n value, may depend upon wavelength and primary, because absorption decreases the extinction free mean path of light, therefore the lateral propagation of light. This idea extends the one introduced by Ino and Berns in Ref. [29] and Rossier and Hersch in Ref. [30] where different (wavelength-independent) n values were attributed to the different inks, fitted from the measured spectral reflectances of halftone patches. In our approach, one spectral n value will be attributed to each primary, computed thanks to close form formulas, and representing an average number of backscattering events in the print. In the equations hereinafter, all reflectances and n values are spectral parameters, even though the dependence upon wavelength is not specified in order to keep the equations easier to read.

Let us now introduce the model, by considering first a solid primary (surface coverage 1). Even though the Yule-Nielsen effect is not visible with this solid primary, there is lateral light propagation in it, that can be represented by n_i back-scattering events in average. Each back-scattering event concerns a fraction r of light. After the n_i scattering events, the final reflectance (which has been previously measured) is R_i (Fig. 3-a and 3-b):

$$r^{n_i} = R_i \tag{20}$$

It follows from Eq. (20) that

$$r = R_i^{1/n_i} \tag{21}$$

therefore that the fraction of light concerned by each scattering event in this primary is R_i^{1/n_i}.

If we extend this line of reasonning to a halftone color of one ink, therefore containing two primaries (Fig. 3-c): the unprinted support labeled 1, and the ink labeled i, with respective surface coverages a_1 and $a_i = 1 - a_1$, we must consider the fact that back-scattering events occur in the two primaries. We assume that each backscattering event has a probability a_1 to occur in primary 1, and a probability a_i to occur in primary i; the average fraction of light concerned is

$$r = a_1 R_1^{1/n_1} + a_i R_i^{1/n_i} \tag{22}$$

Since we have n backscattering events distributed in primaries 1 and i according to the respective probabilities a_1 and a_i, the total number of backscattering events is, in average,

$$n = a_1 n_1 + a_i n_i \tag{23}$$

It comes after Eqs. (22) and (23) that the reflectance of the halftone patch is

$$R = r^n = \left[a_1 R_1^{1/n_1} + a_i R_i^{1/n_i}\right]^{a_1 n_1 + a_i n_i} \quad (24)$$

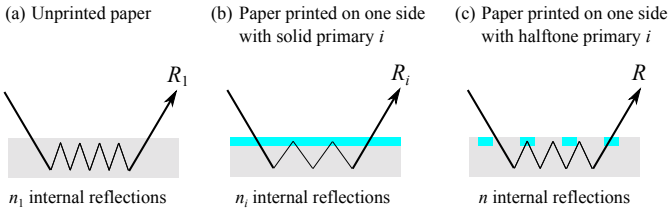

Fig. 3. Internal reflections undergone by light before being reflected in the case of (a) an unprinted paper, (b) a printed paper with a solid primary layer and (c) a halftone print.

The average numbers of internal reflections n_1 and n_i are calculated according to the method described in Section 3, from the reflectance and transmittance of half-layers that we propose to determine now.

Regarding the unprinted paper, it is considered as a symmetrical diffusing layer whose transfer factors R_1 and T_1 are measured. The unprinted paper sheet is then represented by the following transfer matrix:

$$\mathbf{M}_{11} = \frac{1}{T_1}\begin{pmatrix} 1 & -R_1 \\ R_1 & T_1^2 - R_1^2 \end{pmatrix} \quad (25)$$

We suppose now that the sheet of paper is the superposition of two identical symmetrical half-layers having both half the thickness of the sheet, and whose transfer matrix $\mathbf{A}_{11}$ satisfies the relation (see Fig. 4-a):

$$\mathbf{A}_{11}^2 = \mathbf{M}_{11} \quad (26)$$

Note that the number of sublayers could be 3 or more but there is no analytical formula giving the average number of internal reflections for more than 2 sublayers, and the advantage of the model (i.e. the fact that it is based on analytical formulas) vanishes.

We denote as ρ_1 and τ_1 the transfer factors associated with the matrix $\mathbf{A}_{11}$, i.e. the transfer factors of a half-layer:

$$\mathbf{A}_{11} = \frac{1}{\tau_1}\begin{pmatrix} 1 & -\rho_1 \\ \rho_1 & \tau_1^2 - \rho_1^2 \end{pmatrix} = \mathbf{M}_{11}^{1/2} \quad (27)$$

The transfer factors ρ_1 and τ_1 of the half-layer are obtained by applying Eqs. (6) and (7), respectively, to matrix $\mathbf{M}_{11}^{1/2}$. Note that since the half-layer is symmetrical, similar values for ρ_1 and τ_1 would be given by formulas (8) and (9). From Eq. (**??**) in which $\rho_1' = \rho_2 = \rho_1$, we obtain the average number of reflections between the two identical half-layers:

$$n_1 = \frac{1+\rho_1^2}{1-\rho_1^2} \quad (28)$$

At this step of the line of reasonning, ρ_1 and τ_1, and thus n_1, are just numerical values but it is more interesting that the latter are closed-form expressions as functions of the measured transfer factors R_1 and T_1 of the unprinted paper. For this, it is necessary to develop formulas (6) to (9) applied to matrix $\mathbf{M}_{11}^{1/2}$ [see Eq. (27)]. But these developments require many calculations which involves the diagonalization of the matrix $\mathbf{M}_{11}$. Therefore, we propose to present, in the following, an equivalent but simpler method based on the inversion of the Kubelka formulas leading to the average number of internal reflections n_1 as a simple closed-form expression in terms of R_1 and T_1.

The Kubelka formulas (10) and (11) applied to the superposition of the two identical symmetrical half-layers give:

$$R_1 = \rho_1 + \frac{\rho_1 \tau_1^2}{1-\rho_1^2} \quad (29)$$

and

$$T_1 = \frac{\tau_1^2}{1-\rho_1^2} \quad (30)$$

We deduce the reflectance ρ_1 and the tansmittance τ_1 of one half-layer by inversing Eqs. (29) and (30):

$$\rho_1 = \frac{R_1}{1+T_1} \quad (31)$$

$$\tau_1 = \frac{\sqrt{T_1\left[(1+T_1)^2 - R_1^2\right]}}{1+T_1} \quad (32)$$

Finally, according to Eqs. (28) and (31), the average number of internal reflections expressed in terms of the measured reflectance and transmittance of the unprinted paper is:

$$n_1 = 1 + \frac{2R_1^2}{(1+T_1)^2 - R_1^2} \quad (33)$$

The average number of internal reflections n_i in the sheet printed with the solid primary i is computed in the same way. The transfer factors of the print, denoted as R_i, R_i', T_i and T_i', are measured. It is then possible to build the corresponding transfer matrix:

$$\mathbf{M}_{i1} = \frac{1}{T_i}\begin{pmatrix} 1 & -R_i' \\ R_i & T_i T_i' - R_i R_i' \end{pmatrix} \quad (34)$$

It is assumed that the print is the superposition of a non-symmetric diffusing half-layer with the solid primary i, whose transfer matrix is denoted $\mathbf{A}_{i1}$, and of the symmetric unprinted half-layer, whose transfer matrix remains $\mathbf{A}_{11} = \mathbf{M}_{11}^{1/2}$ (see Fig. 4-b). Hence, we have:

$$\mathbf{M}_{i1} = \mathbf{A}_{i1}.\mathbf{A}_{11} \quad (35)$$

The transfer factors associated with $\mathbf{A}_{i1}$ are denoted as ρ_i, ρ_i', τ_i and τ_i':

$$\mathbf{A}_{i1} = \frac{1}{\tau_i}\begin{pmatrix} 1 & -\rho_i' \\ \rho_i & \tau_i\tau_i' - \rho_i\rho_i' \end{pmatrix} = \mathbf{M}_{i1}.\mathbf{A}_{11}^{-1} \quad (36)$$

The transfer factors ρ_i, τ_i, ρ_i' and τ_i' of the non-symmetric half-layer with the solid primary i are obtained by applying Eqs. (6) to (9), respectively, to matrix $\mathbf{M}_{i1}.\mathbf{A}_{11}^{-1}$. The average number of internal reflections n_i between the printed and unprinted half-layers is obtained by applying Eq. (18) in which r_1' is replaced with ρ_i' and r_2 with ρ_1:

$$n_i = \frac{1+\rho_i'\rho_1}{1-\rho_i'\rho_1} \quad (37)$$

It is also possible to obtain n_i as a closed-form expression in terms of the transfer factors R_1 et T_1 of the unprinted paper, and the back-side reflectance R'_i of the paper with the solid primary i. For this, we use the Kubelka formula (12) applied to the superposition of the printed and unprinted half-layers:

$$R'_i = \rho_1 + \frac{\rho'_i \tau_1^2}{1 - \rho_1 \rho'_i} \tag{38}$$

We deduce the reflectance ρ'_i of the printed half-layer by inversing Eq. (38):

$$\rho'_i = \frac{R'_i - \rho_1}{\tau_1^2 + \rho_1 \left(R'_i - \rho_1\right)} \tag{39}$$

Then, we replace ρ_1 and τ_1 with their expressions given by Eqs. (31) and (32), respectively, and obtain:

$$\rho'_i = \frac{(1+T_1)\left[R'_i(1+T_1) - R_1\right]}{T_1\left[(1+T_1)^2 - R_1^2\right] + R_1\left[R'_i(1+T_1) - R_i\right]} \tag{40}$$

Finally, according to Eqs. (31), (37) and (40), the average number of internal reflections n_i expressed in terms of the measured reflectance and transmittance of the paper printed with primary i can be written:

$$n_i = 1 + \frac{2R_1\left[R'_i(1+T_1) - R_1\right]}{T_1\left[(1+T_1)^2 - R_1^2\right]} \tag{41}$$

We recall that the transfer factors R_1, R'_i and T_1, thereby parameters n_1 and n_i, depend on wavelength. We notice that n_i depends only on the reflectance R_1 and the transmittance T_1 of the paper as well as on the back-side reflectance of the primaries R'_i which is the measured reflectance of the unprinted side of the paper, the other side being printed with fulltone primary i. One also remarks that the use of transfer matrices is not necessary to justify the formulas of the MPD-YN model since these latter have been deduced from the Kubelka formulas [see Eqs. (29), (30) and (38)] and their inversion [see Eqs. (31), (32) and (39)]. However, we will see in Section 6 that the transfer matrix approach will be very useful for the predictions of recto-verso halftone color prints.

In the case of an opaque paper, the influence of the solid primary ink layer on the back-side reflectance R'_i is quite negligeable. This latter is therefore similar to the reflectance R_1 of the unprinted paper. It follows that the average numbers of internal reflections n_i are identical for all the primaries and equal to n_1. Thus, according to (23) and (24), the reflectance factor of the halftone print can be written:

$$R = \left[(1-a_i)\, R_1^{1/n_1} + a_i R_i^{1/n_1}\right]^{n_1} \tag{42}$$

where n_1 is given by Eq. (33).

We retrieve the formula of the Yule-Nielsen model where the n parameter here is a spectral parameter calculated from the measured transfer factors R_1 and T_1 of the unprinted paper. In this case, the calibration of the MPD-YN model for reflectance predictions requires the same number of measurements as for the Yule-Nielsen model, namely the front-side reflectance factors R_i of all the solid Neugebauer primaries, to which is added the measurement of the transmittance T_1 of the unprinted paper, necessary to calculate the number of internal reflections n_1 according to Eq. (33).

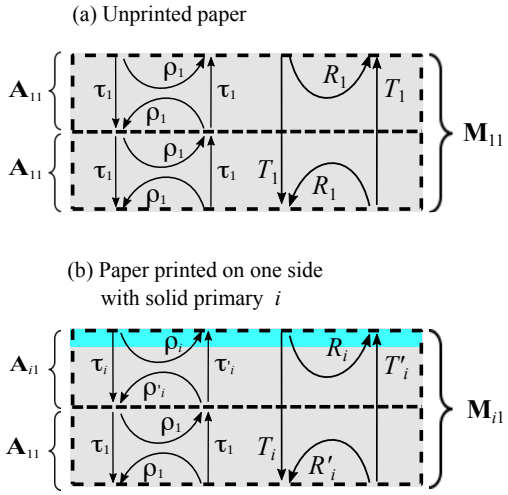

Fig. 4. Separation of the print, (a) without ink and (b) with solid primary, into two half-layers.

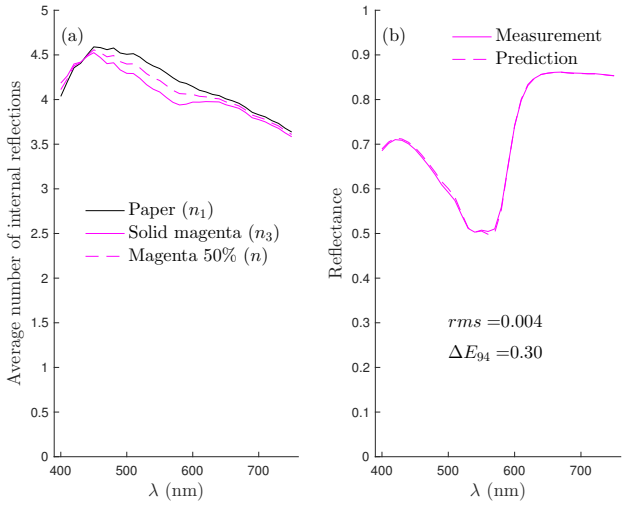

Fig. 5. a) Spectral values of the average number of internal reflections within a symmetrical paper sheet being either unprinted (black solid line), printed with a solid magenta ink layer (magenta solid line) or printed with a 0.5 surface coverage halftone of magenta ink (magenta dashed line); (b) Spectral reflectances of the 0.5 surface coverage halftone of magenta ink as measured and predicted by Eq. (24).

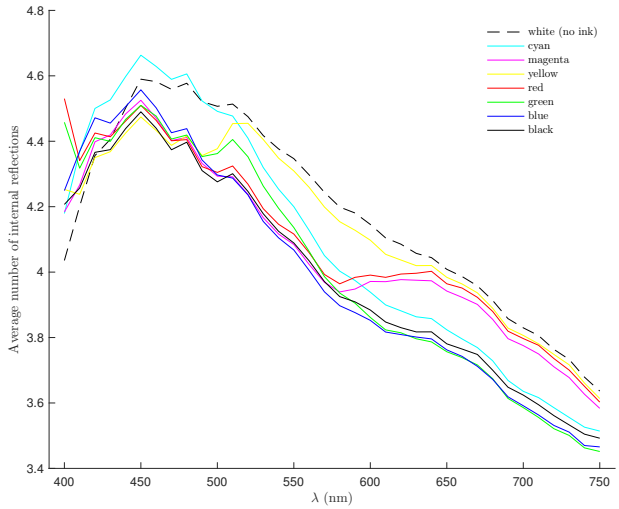

Fig. 6. Spectral values of the average numbers of internal reflections within a symmetrical paper sheet printed with each of the eight solid Neugebauer primaries.

In order to visualize the spectral values taken by the average numbers of internal reflections in the case of real prints, we printed a halftone of magenta ink with a nominal surface coverage of 0.5 on symmetrical, supercalendered, nonfluorescent paper APCO. Figure 5-a represents the average number of internal reflections undergone by light within the blank support (n_1), within the solid magenta print (n_3) and within the halftone print (n). The average number values, calculated using the formula (18), are around 4. Their variation according to the wavelength of light is noticeable, but similar variations are observed from one sample to another one. The solid curve, associated with the solid ink, is located beneath the dashed curve, associated with the halftone: we logically deduce that the light is less reflected as the ink layer is more absorbing. Figure 6 represents the average number of internal reflections undergone by light within APCO paper printed with each of the eight solid Neugebauer primaries.

The spectral reflectance of the halftone print is calculated (see Fig. 5-b) using Eq. (24). The root mean square deviation *rms* and the CIELAB ΔE_{94} color difference between the predicted and measured spectra are respectively 0.004 and 0.30. With the Yule-Nielsen model, these values are equal to 0.003 and 0.17 respectively, with a fitted value $n = 2.6$ and an effective surface coverage $a_3 = 0.54$. In this example, the predictions are good whatever the model is: in both cases the color difference is clearly lower than 1. However, we notice the advantage of the MPD-YN model for which the terms n_1 and n_3 are calculated thanks to Eqs. (33) and (41) respectively, in contrast with the parameter n of the Yule-Nielsen model which is fitted so as to minimize the differences between predicted and measured spectra.

The MPD-YN model is not limited to predictions for single-ink halftone colors: Eq. (24) can be generalized to halftone prints involving the eight Neugebauer primaries with any coverage a_i; in this case the front-side reflectance factors is written:

$$R = \left[\sum_{i=1}^{8} a_i R_i^{1/n_i}\right]^n \tag{43}$$

with

$$\sum_{i=1}^{8} a_i = 1, \tag{44}$$

$$n = \sum_{i=1}^{8} a_i n_i \tag{45}$$

and n_i is given by Eq. (41).

Even if the back-side reflectance, R' (on the unprinted side) is not interesting in the case of a single-sided halftone print, it can also be predicted thanks to the following formulas:

$$R' = \left[\sum_{i=1}^{8} a_i R_i'^{1/n_i}\right]^n \tag{46}$$

where R_i' is the back-side reflectance measured on the single-sided print with the solid Neugebauer primary i; the spectral terms n_i and n are given by the formulas (41) and (45) respectively.

5. MPD-YN MODEL IN TRANSMITTANCE MODE

Regarding the transmittance of the print, the average number of internal reflections is equal to the one calculated for the reflectance, minus 1 (see Fig. 7). By following similar line of reasonning as for the reflectance, we can express the transmittance T_j ($j = 1$ in the case of paper without ink or $j = i$ in the case of a solid primary i) as the result of $n_j - 1$ events of factor $T_j^{1/(n_j-1)}$:

$$T_j = \left(T_j^{1/(n_j-1)}\right)^{n_j-1} \tag{47}$$

The transmittance T of the halftone print considered above results from n' successive attenuations of the light, each of factor t, such as:

$$T = t^{n'} \tag{48}$$

with

$$t = (1 - a_i)\, T_1^{1/(n_1-1)} + a_i T_i^{1/(n_i-1)} \tag{49}$$

and

$$n' = (1 - a_i)\,(n_1 - 1) + a_i\,(n_i - 1) \tag{50}$$

where n_1 and n_i are given by Eqs. (33) and (41) respectively. We thus obtain:

$$T = \left[(1 - a_i)\, T_1^{1/(n_1-1)} + a_i T_i^{1/(n_i-1)}\right]^{(1-a_i)n_1 + a_i n_i - 1} \tag{51}$$

Like the reflectance model, Eq. (51) can be generalized to halftone prints involving the eight Neugebauer primaries with any coverage a_i; in this case, the forward transmittance factors is written:

$$T = \left[\sum_{i=1}^{8} a_i T_i^{1/(n_i-1)}\right]^{n-1} \tag{52}$$

where n_i and n are given by Eqs. (41) and (45) respectively.

The forward transmittance T' (identical to the backward transmittance, more or less measurement error) can also be predicted thanks to the following Eq.:

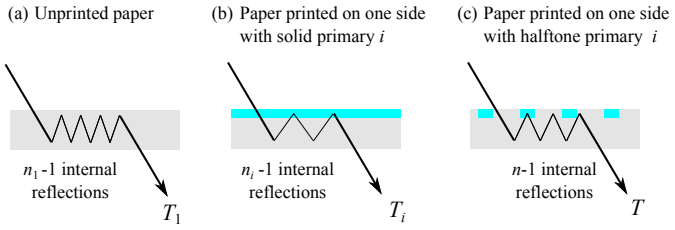

Fig. 7. Internal reflections undergone by light before being transmitted in the case of (a) an unprinted paper, (b) a printed paper with a solid primary layer and (c) a halftone print.

$$T' = \left[\sum_{i=1}^{8} a_i T_i'^{1/(n_i-1)}\right]^{n-1} \tag{53}$$

where T_i' is the forward transmittance measured on the single-sided print with the solid Neugebauer primary i.

6. EXTENSION TO DUPLEX HALFTONE PRINTS

As for the Yule-Nielsen model, extended to double-sided prints in Ref. [15], we propose a version of the MPD-YN model able to predict the reflectance and spectral transmittance factors of prints with halftone colors on their two sides. The prediction method is in two steps: in the first step, the halftone colors printed on the recto and verso sides are both considered as printed on the recto on different areas of the paper sheet, the verso being unprinted; the transfer factors of these two colors patches are predicted and a transfer matrix is attached to each one. In a second step, the two transfer matrices are combined and we can deduce the transfer factors of the paper printed with these two colors printed one on the recto side, the other on the verso side.

Let us present these two steps in detail. In the first step, we denote as A the color on the front side (recto) and B the one on the back side (verso). We consider these two colors printed on the recto side. The transfer factors R_A, R'_A, T_A and T'_A of the color patch A and the ones R_B, R'_B, T_B and T'_B of the color patch B are predicted thanks to the model presented in the previous section [see Eqs. (43), (45), (46), (52) and (53)]. The transfer matrix representing the color patch A (see Fig. 8-b) is:

$$\mathbf{M}_A = \frac{1}{T_A}\begin{pmatrix} 1 & -R'_A \\ R_A & T_A T'_A - R_A R'_A \end{pmatrix} \tag{54}$$

Regarding the color patch B, we now consider that it is printed on the verso side (the recto being unprinted); it is represented by the following transfert matrix $\mathbf{M}_B$ (see Fig. 8-c) where the front-side and back-side reflectances, and the forward and backward transmittances, are mutually exchanged compared to their respective arrangement in $\mathbf{M}_A$:

$$\mathbf{M}_B = \frac{1}{T'_B}\begin{pmatrix} 1 & -R_B \\ R'_B & T_B T'_B - R_B R'_B \end{pmatrix} \tag{55}$$

The spectral measurements of the transfer factors R_1 and T_1 of the unprinted paper (see Fig. 8-a) are used to build the transfer matrix $\mathbf{M}_{11}$ given by Eq. (25).

The second step is the combination of the matrices $\mathbf{M}_{11}$, $\mathbf{M}_A$ and $\mathbf{M}_B$ in order to obtain the transfer matrix of the recto-verso print with the color A on the recto side and the color B on the verso side. For this purpose, we decompose each of the three samples: unprinted paper, color patch A (recto side) and color patch B (verso side), into two half-layers as shown in Fig. 8. In the unprinted paper (matrix $\mathbf{M}_{11}$), the two half-layers are similar and represented by the transfer matrix $\mathbf{M}_{11}^{1/2}$. The color patch A is made of the half-layer with color A (matrix $\mathbf{P}_A$ to be determined) on top of an unprinted half-layer (matrix $\mathbf{M}_{11}^{1/2}$). Since we have

$$\mathbf{M}_A = \mathbf{P}_A.\mathbf{M}_{11}^{1/2}, \tag{56}$$

the transfer matrix representing the upper half-layer is therefore

$$\mathbf{P}_A = \mathbf{M}_A.\mathbf{M}_{11}^{-1/2}. \tag{57}$$

The color patch B is decomposed into an unprinted half-layer (matrix $\mathbf{M}_{11}^{1/2}$) on top of an half-layer with color B. The transfer matrix representing this latter is:

$$\mathbf{P}_B = \mathbf{M}_{11}^{-1/2}.\mathbf{M}_B. \tag{58}$$

Finally, if the paper is printed with the color A on the recto side and the color B on the verso side, we can reasonnably assume that it can be decomposed into the half-layer with the color A, represented by the matrix $\mathbf{P}_A$, on top of the half-layer with color B, represented by the matrix $\mathbf{P}_B$ (see Fig. 8-d). Hence, the transfer matrix of the recto-verso print is given by:

$$\mathbf{M}_{AB} = \mathbf{M}_A.\mathbf{M}_{11}^{-1}.\mathbf{M}_B \tag{59}$$

The transfer factors R_{AB}, R'_{AB}, T_{AB} and T'_{AB} of the recto-verso halftone print can be deduced from the formulas (6) to (9) applied to the matrix $\mathbf{M}_{AB}$. After computation, one obtains:

$$R_{AB} = R_A - \frac{(R_1 - R'_B)\,T_A T'_A}{T_1^2 - (R_1 - R'_A)\,(R_1 - R'_B)} \tag{60}$$

$$T_{AB} = \frac{T_1 T_A T'_B}{T_1^2 - (R_1 - R'_A)\,(R_1 - R'_B)} \tag{61}$$

$$R'_{AB} = R_B - \frac{(R_1 - R'_A)\,T_B T'_B}{T_1^2 - (R_1 - R'_A)\,(R_1 - R'_B)} \tag{62}$$

$$T'_{AB} = \frac{T_1 T'_A T_B}{T_1^2 - (R_1 - R'_A)\,(R_1 - R'_B)} \tag{63}$$

7. CALIBRATION

The calibration of the Mean-Path-Defined Yule-Nielsen model for recto-verso halftone color prints in reflectance mode needs the measurements of the front-side reflectances R_i and back-side reflectances R'_i of all the Neugebauer primaries, and the transmittance of the unprinted paper T_1. In transmittance mode, the forward transmittances T_i and backward transmittances T'_i of all Neugebauer primaries must be added. Note that for reflectance predictions of halftone colors printed on one side of an opaque paper sheet, the MPD-YN model needs the measurements of the front-side reflectances R_i for all Neugebauer primaries and the transmittance of the unprinted paper T_1, namely one more measurement than for the calibration of the Yule-Nielsen model.

Moreover, in the case of halftone prints, it is known that the problem of dot gain needs additionnal measurements, in reflectance mode if one wants to predict reflectances, and/or transmittance mode if one wants to predict transmittances. At printing time, the inks spread on the substrate in a more or less

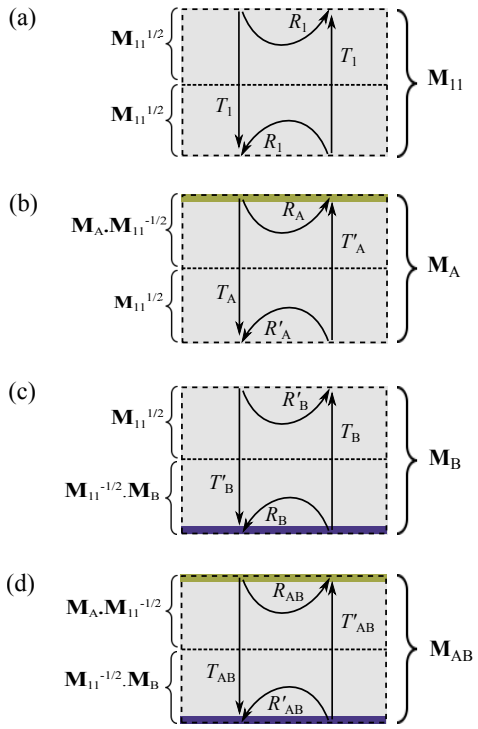

Fig. 8. Modeling a duplex halftone print (d) from two single-sided halftone prints (b) and (c), and the unprinted paper (a).

pronounced way according to the physicochemical and mechanical properties of the materials. This phenomenon of spreading is called "mechanical dot gain". The combined effects of optical dot gain (Yule-Nielsen effect) and mechanical dot gain imply that actual coverages, called "effective coverages", are different from the coverages defined in the digital layout, called "nominal coverages". The effective coverages are the input parameters of the color prediction models but they are difficult to measure independently of the models, despite attempts using heavy methods to implement such as microscopic image analysis coupled with a model of optical dot gain [28, 31, 32]. An alternative to these methods is to make an assessment of the effective coverages using a macroscopic method that combines measurements of the transfer factors of 36 halftone samples and the use of the model itself [13]. We propose to present in detail this method. The general principle of the method is to build correction curves relating the nominal and effective coverages of cyan, magenta and yellow inks, taking into account that the spreading of a given ink can be done in a different way on paper, depending on whether the latter is non-inked or printed with a solid Neugebauer primary composed with the other two inks. First, a set of 36 halftone color samples, shown in Fig. 9, is printed on one side of the symmetric paper sheet. These samples correspond to all the possible combinations of a given ink u of nominal coverage a equal to 0.25, 0.50 or 0.75, and a solid primary v obtained with the inks other than u. For example, for cyan ink, the 12 halftone colors $(c-m-j)$, represented in Table 1, are obtained.

There are also 12 samples for magenta and 12 samples for yellow. Each of these halftone colors contains two primaries which correspond to areas where the primary v is alone and areas where the ink u is superposed on the primary v to obtain the primary $u+v$. We denote by x the effective coverage of the primary $u+v$. We measure the spectral reflectance $R_{u/v}^{(m)}(\lambda)$

Table 1. List of halftone colors used to estimate the mechanical dot gain of the cyan ink.

cyan/white	$(0.25-0-0)$	$(0.50-0-0)$	$(0.75-0-0)$
cyan/magenta	$(0.25-1-0)$	$(0.50-1-0)$	$(0.75-1-0)$
cyan/yellow	$(0.25-0-1)$	$(0.50-0-1)$	$(0.75-0-1)$
cyan/red	$(0.25-1-1)$	$(0.50-1-1)$	$(0.75-1-1)$

and the spectral transmittance $T_{u/v}^{(m)}(\lambda)$ of this halftone color. We denote by $R_{u/v}^{(x)}(\lambda)$ and $T_{u/v}^{(x)}(\lambda)$ the theoretical reflectance and theoretical transmittance associated with this color and calculated using a color prediction model. The effective coverage is the value that minimizes the CIELAB ΔE_{94} color distance between the measured spectrum and the spectrum predicted by the considered model when the parameter x varies between 0 and 1. We then obtain a value $\tilde{a}_{u/v}^{(R)}$ for the effective coverage in reflectance mode:

$$\tilde{a}_{u/v}^{(R)} = \underset{0\leq x\leq 1}{argmin}\Delta E_{94}\left(R_{u/v}^{(m)}(\lambda),\, R_{u/v}^{(x)}(\lambda)\right) \qquad \textbf{(64)}$$

and generally a different value $\tilde{a}_{u/v}^{(T)}$ in transmittance mode [11]:

$$\tilde{a}_{u/v}^{(T)} = \underset{0\leq x\leq 1}{argmin}\Delta E_{94}\left(T_{u/v}^{(m)}(\lambda),\, T_{u/v}^{(x)}(\lambda)\right) \qquad \textbf{(65)}$$

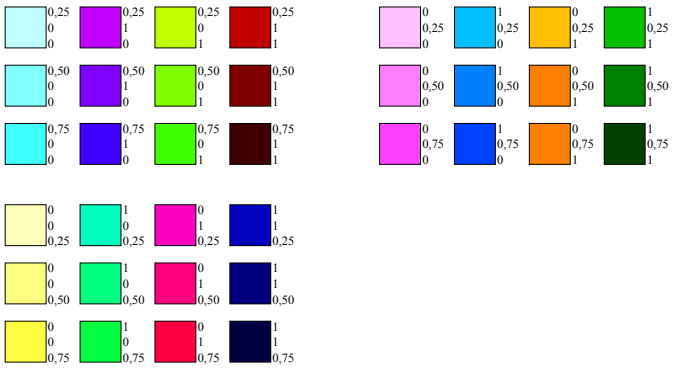

Fig. 9. Color samples for calibration of halftone color prediction models (the three values at the right of each color squares are respectively the c, m and y values).

Thus, for each couple ink u, primary v, one obtain three effective coverages corresponding to the three nominal coverages 0.25, 0.50 and 0.75. By linear interpolation, one creates a function $f_{u/v}$, also called ink spreading curve [13], establishing the correspondance between the nominal and effective surface coverages. More precisely, $f_{u/v}(a)$ gives the effective coverage of the ink u on the primary v for any nominal coverage a. Considering the 36 calibration samples, one obtains a set of four spreading curves for each ink, therefore a total of 12 spreading curves for one given mode (reflectance or transmittance).

Once the spreading curves in reflexion mode (or transmission mode) have been obtained, it is then possible to predict the spectral reflectance (respectively, transmittance) of any halftone color printed with the inks and paper used for the calibration. More precisely, if we consider a halftone color whose nominal coverages of cyan, magenta and yellow inks are denoted c_0, m_0

and y_0 respectively, then the latter are converted to effective coverages c, m and y by performing a few iterations on the following three equations:

$$\begin{aligned} c &= (1-m)(1-y) f_{c/w}(c_0) + m(1-y) f_{c/m}(c_0) + \\ &\quad (1-m) y f_{c/y}(c_0) + myf_{c/m+y}(c_0) \\ m &= (1-c)(1-y) f_{m/w}(m_0) + c(1-y) f_{m/c}(m_0) + \\ &\quad (1-c) y f_{m/y}(m_0) + cyf_{m/c+y}(m_0) \\ y &= (1-c)(1-m) f_{y/w}(y_0) + c(1-m) f_{y/c}(y_0) + \\ &\quad (1-c) m f_{y/m}(y_0) + cmf_{y/c+m}(y_0) \end{aligned} \tag{66}$$

The effective coverages of the three inks are obtained by calculating the average of their four spreading curves, weighted by the coverages of the primaries over which these halftone inks overlap: for example, the weight associated with the curve of cyan ink on the red primary (i.e. $f_{c/m+y}$) is equal to the coverage of the red primary, that is to say my. At the first iteration, the initial values to the right of the equations (66) are $c = c_0$, $m = m_0$ and $y = y_0$, the values of c, m and y obtained on the left are then plotted in right-hand side of the equations (66) which give new values of c, m and y, and so on, until the values of c, m and y stabilize. These last values are then plotted in the Demichel equations (1) in order to obtain the effective coverages $a_i, i = 1, ..., 8$ of the eight Neugebauer primaries.

8. PREDICTION ACCURACY

We tested the performance of the Mean-Path-Defined Yule-Nielsen model for the reflectance prediction of 81 color samples printed on one side of an APCO paper sheet (symmetrical, super-calendered and non-fluorescent), the other side being unprinted, with a classical rotated cluster halftoning at 120 lpi, with ink densities of 0.72 for cyan, 0.58 for magenta and 0.82 for yellow. The assessment of the mechanical dot gain was established by using the optimization formulas (64) and (65) applied to the 36 calibration samples (see Section 7) printed on the same sheet of paper as the 81 test samples. The reflectance factor of each sample is measured with the X-rite Color i7 spectrophotometer with a geometry d:8°. It is assumed that APCO paper is opaque enough to use Eq. (42) for predicting the spectral reflectance factors of the 81 color samples, randomly selected, exclusing the halftone colors used for the calibration of the model. The transmittance factor T_1 of the unprinted paper, involved in the calculation of the average number of internal reflection n_1 [see Eq. (33)], is measured with a geometry d:0°. The precision of the predictions is evaluated (see Table 2) by calculating the average of the root mean square (rms) spectral differences and the average of the CIELAB ΔE_{94} color distances, over the 81 test samples, between predicted and measured spectra. We also write into brackets the 95th percentile of the CIELAB ΔE_{94} distances (Q95). The results obtained with the MPD-YN model are compared with the ones obtained with the Yule-Nielsen model, whose ink surface coverages and n value have been calibrated independently of the MPD-YN model: the constant n value, fitted from the 36 calibration samples, was 4.5 for the prediction of the reflectance factors. Good accuracy have been observed for both the MPD-YN model and the Yule-Nielsen model: the mean square deviations are less than one percent and the colorimetric deviations are less than 1. However, even though equivalent performances are observed, the drawback with the Yule-Nielsen model is that the value of the n parameter must be fitted before allowing predictions. Recall that the MPD-YN model computes one spectal n value for each halftone color. One example of spectral n value is displayed in Figure 5, corresponding to the magenta 50 % halftone patch, printed with the same setup and materials than the set of halftone colors tested in this experiment.

Table 2. Prediction accuracy of the MPD-YN and Yule-Nielsen models on 81 halftone colors printed on one side of an APCO paper sheet with the Canon Pro9500 inkjet printer.

$rms - \Delta E_{94}$ (Q95) *	
Model	Reflectance
MPD-YN	0.006 – 0.53 (1.18)
Yule-Nielsen	0.006 – 0.49 (1.10)

*average of rms – average of ΔE_{94} (95^{th} percentile)

We also tested the performance of the MPD-YN model on 36 different duplex halftone color samples printed on APCO paper with a classical rotated cluster halftoning at 120 lpi, with ink densities of 0.60 for cyan, 0.45 for magenta and 0.55 for yellow. The precision of the predictions is presented in Table 3. The results obtained with the MPD-YN model are compared with those obtained with the Yule-Nielsen model with the parameter $n = 2.3$ for the predictions of the reflectance factors and $n = 1.6$ for the predictions of the transmittance factors (these two n-values, rather low as expected in case of low ink densities [9], were fitted using the 36 calibration samples). We observe good accuracy for both the MPD-YN model and the Yule-Nielsen model: the mean square deviations are less than one percent and the colorimetric deviations are less than 1.

Finally, we tested the performance of the MPD-YN model on 78 duplex halftone samples printed on office paper with a classical rotated cluster halftoning at 150 lpi. The results, shown in Table 4, are a little bit less accurate than the ones obtained with APCO paper but they are similar for both MPD-YN and Yule-Nielsen models with mean square deviations lower than 1.5 percent and colorimetric deviations lower than 1.5 in average.

Table 3. Prediction accuracy of the MPD-YN and Yule-Nielsen models on 36 duplex halftone colors printed on an APCO paper sheet with the Canon Pro9500 inkjet printer.

$rms - \Delta E_{94}$ (Q95) *		
Model	Reflectance	Transmittance
MPD-YN	0.007 – 0.76 (1.58)	0.001 – 0.94 (1.49)
Yule-Nielsen	0.007 – 0.70 (1.36)	0.002 – 0.94 (1.39)

*average of rms – average of ΔE_{94} (95^{th} percentile)

9. CONCLUSION

We have introduced a surface model, called MPD-YN model, allowing the predictions of the spectral reflectances and transmittances of single-sided and duplex halftone prints, and whose formulation is close to the one of the Yule-Nielsen model. This model describes the optical dot gain by introducing into the

Table 4. Prediction accuracy of the MPD-YN and Yule-Nielsen models on 78 duplex halftone colors printed on an office paper sheet with the Canon Pro9500 inkjet printer.

$rms - \Delta E_{94}$ (Q95) *		
Model	Reflectance	Transmittance
MPD-YN	$0.012 - 1.27\ (2.77)$	$0.004 - 1.17\ (2.14)$
Yule-Nielsen	$0.013 - 1.16\ (3.11)$	$0.003 - 1.33\ (2.05)$

*average of rms – average of ΔE_{94} (95^{th} percentile)

Neugebauer formula spectral terms related to the concept of average number of internal reflections between two half-layers. The advantage of the MPD-YN model is that these terms, wavelength-dependent and different for each halfone, are calculated from the measured transfer factors (reflectances, transmittances) of the solid Neugebauer primaries printed on the paper; they are not free parameters, in contrast with the n parameter of the Yule-Nielsen model which is fitted during the calibration phase by minimizing the differences between the predicted and measured spectra on a certain number of samples. The replacement of the free n parameter by this computed parameter has been possible thanks to the spectral information carried by the transmittance of the solid primary patches, measured in addition to the spectral reflectances. The spectral n parameter in the MPD-YN model is mainly related to the optical properties of the paper (scattering and absorption). When the paper is opaque enough so that the inks printed on the recto-side are not visible on the verso side, the back-side reflectances of the paper printed with the solid primaries are similar and the n parameter depends only on the spectral reflectance and transmittance of the unprinted paper. In the general case, through the back reflectances of the solid primary patches, the n parameter can render the effects of the paper's translucency or the fact that its optical properties are modified when the inks penetrate into it. The predictions given by the MPD-YN model are as accurate as the ones given by the Yule-Nielsen model (Yule-Nielsen modified spectral Neugebauer model).

REFERENCES

1. V. Babaei, R.D. Hersch, Yule-Nielsen based multi-angle reflectance prediction of metallic halftones, Proc. SPIE 9395, paper 93950H (2015).
2. P. Pjanic, R. D. Hersch, Specular color imaging on a metallic substrate, Proc. IS&T 21st Color and Imaging Conference, 61–68 (2013).
3. M. Hébert, D. Nébouy, S. Mazauric, Color and spectral mixing in printed surfaces, LNCS 9016 Computational Color Imaging Workshop, 3–15 (2015).
4. S. Mazauric, T. Fournel, M. Hebert, Fast-calibration reflectance-transmittance model to compute multiview recto-verso prints, Proceedings of the 6th International Workshop CCIW, 223–232, Milano (2017).
5. N. Dalloz, S. Mazauric, T. Fournel, M. Hébert, How to design a recto-verso print displaying different images in various everyday-life lighting conditions, IS&T Electronic Imaging Symposium, Materials Appearance, Burlingame (2017).
6. G. L. Rogers, The Point Spread Function and Optical Dot Gain, in Handbook of Digital Imaging, Vol. 2, Ed. Mickael Kriss, Wiley, pp. 1133—1164 (2015).
7. J.A.C. Yule, W.J. Nielsen, The penetration of light into paper and its effect on halftone reproduction, Proc. TAGA **3**, 65–76 (1951).
8. J. A. S. Viggiano, The color of halftone tints, Proc. TAGA, 647–661 (1985)
9. M. Hébert, R. D. Hersch, Review of spectral reflectance prediction models for halftone prints: calibration, prediction and performance, Color Res. Appl., Vol. 40, pp. 383–397, paper 21907 (2015).
10. F. R. Clapper, J. A. C. Yule, The effect of multiple internal reflections on the densities of halftones prints on paper, J. Opt. Soc. Am. **43**, 600–603 (1953).
11. S. Mazauric, M. Hébert, L. Simonot, T. Fournel, Two-flux transfer matrix model for predicting the reflectance and transmittance of duplex halftone prints, J. Opt. Soc. Am. **31**, 2775–2788 (2014).
12. M. Hébert, F. Emmel, Two-flux and multiflux matrix models for colored surfaces, in Handbook of Digital Imaging, Mickael Kriss Ed., John Wiley & Sons, pp. 1233–1277 (2015).
13. R. D. Hersch, F. Crété, Improving the Yule-Nielsen modified spectral Neugebauer model by dot surface coverages depending on the ink superposition conditions, Proc SPIE 5667, 434–445 (2005).
14. M. E. Demichel, Procédés **26**, 17–21 (1924).
15. M. Hébert, R. D. Hersch, Yule-Nielsen based recto-verso color halftone transmittance prediction model, J. Opt. Soc. Am. A **50**, 519–525 (2011).
16. J. Machizaud, M. Hébert, Spectral reflectance and transmitance prediction model for stacked of transparency and paper both printed with halftone colors, J. Opt. Soc. Am. A **29**, 1537–1548 (2012).
17. A. Lewandowski, M. Ludl, G. Byrne, G. Dorffner, Applying the Yule-Nielsen equation with negative n, J. Opt. Soc. Am. A **23**, 1827–1834 (2006).
18. J. A. S. Viggiano, Physical significance of negative Yule-Nielsen n-value, Proc. ICIS International Congress of Imaging Science, 607–610 (2006).
19. J. A. S. Viggiano, Ink penetration, isomorphic colorant mixing and negative values of Yule-Nielsen n, Proc. IS & T 18th Color and Imaging Conference, 285–290 (2010).
20. M. Hébert, R. D. Hersch, Analysing halftoning dot blurring by extended spectral prediction models, J. Opt. Soc. Am. A **27**, 6–12 (2010).
21. J. S. Arney, A probability description of the Yule-Nielsen effect. I : Tone reproduction and image quality in the graphic arts, J. Im. Sci. Technol. **41**, 633–636 (1997).
22. J. S. Arney, A probability description of the Yule-Nielsen effect. II : The impact of halftone geometry, Recent Progress in Digital Halftoning II, 456–461 (1999).
23. G. Rogers, Optical dot gain : lateral scattering probabilities, J. Imaging Sci. Technol. **42**, 495–500 (1998).
24. F. R. Ruckdeschel, O. G. Hauser, Yule-Nielsen effect in printing : a physical analysis, Appl. Opt. **17**, 3376–3383 (1978).
25. G. L. Rogers, Effect of light scatter on halftone color, J. Opt. Soc. Am. A **15**, 1813—1821 (1998).
26. G. L. Rogers, A Generalized Clapper–Yule Model of Halftone Reflectance, Color Res. Appl. **25**, 402—407 (2000).
27. P. Kubelka, New contributions to the optics of intensely light-scattering materials, part II: Non homogeneous layers, J. Opt. Soc. Am. **44**, 330–335 (1954).
28. M. Ukishima, Prediction and evaluation of color halftone print quality based on microscopic measurement, Ph. D. dissertation, University of Eastern Finland (2010).
29. K. Ino, R.S. Berns, Building color management modules using linear optimization II. Prepress system for offset printing, J. Imag. Sci. Tech., 42, 99 –114 (1998).
30. R. Rossier, R.D. Hersch, Ink-dependent n-factors for the Yule-Nielsen modified spectral Neugebauer model, Fifth European Conference on Color in Graphics, Imaging and Vision (CGIV), Joensuu, Finland, June 14-18 (2010).
31. G. M. A. Rahaman, O. Norberg, P. Edström, Microscale halftone color image analysis: perspective of spectral color prediction modeling. Proc. SPIE 9015, Paper 901506 (2014).
32. D. Nyström, High Resolution Analysis of Halftone Prints : A Colorimetric and Multispectral Study, PhD dissertation, Linköping University, Sweden (2009).